Article

# The Role of Mesopores in Intracrystalline Transport in USY Zeolite: PFG NMR Diffusion Study on Various Length Scales

P. Kortunov, S. Vasenkov, J. Krger, R. Valiullin, P. Gottschalk, M. F Ela, M. Perez, M. Stcker, B. Drescher, G. McElhiney, C. Berger, R. Glser, and J. Weitkamp

*J. Am. Chem. Soc.*, **2005**, 127 (37), 13055-13059• DOI: 10.1021/ja053134r • Publication Date (Web): 26 August 2005



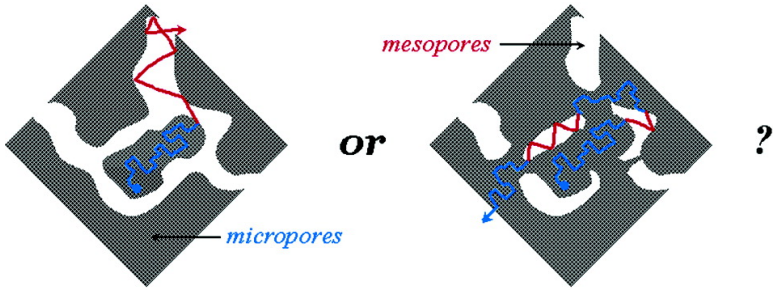


## More About This Article

Additional resources and features associated with this article are available within the HTML version:

- Supporting Information
- Links to the 9 articles that cite this article, as of the time of this article download
- Access to high resolution figures
- Links to articles and content related to this article
- Copyright permission to reproduce figures and/or text from this article

View the Full Text HTML

J|A|C|S
ARTICLES
Published on Web 08/26/2005

# The Role of Mesopores in Intracrystalline Transport in USY Zeolite: PFG NMR Diffusion Study on Various Length Scales

P. Kortunov,[†] S. Vasenkov,*[,†] J. Kärger,[†] R. Valiullin,[†] P. Gottschalk,[†] M. Fé Elía,[‡] M. Perez,[‡] M. Stöcker,[§] B. Drescher,[||] G. McElhiney,[||] C. Berger,[⊥] R. Gläser,[⊥] and J. Weitkamp[⊥]

*Contribution from the Fakultät für Physik und Geowissenschaften, Universität Leipzig, Linnéstrasse 5, D-04103 Leipzig, Germany, Cepsa Research Center, Picos de Europa, 7 Poligono Industrial San Fernando de Henares II, 28850 San Fernando de Henares, Spain, Department of Hydrocarbon Process Chemistry, SINTEF Materials and Chemistry, P.O. Box 124 Blindern Forskningsveien 1, N-0314 Oslo, Norway, Grace GmbH & Co. KG, In Der Hollerhecke 1, D-67545 Worms, Germany, and Institute of Chemical Technology, University of Stuttgart, D-70550 Stuttgart, Germany*

Received May 13, 2005; E-mail: svasenkov@che.ufl.edu

***Abstract:*** PFG NMR has been applied to study intracrystalline diffusion in USY zeolite as well as in the parent ammonium-ion exchanged zeolite Y used to produce the USY by zeolite steaming. The diffusion studies have been performed for a broad range of molecular displacements and with two different types of probe molecules (*n*-octane and 1,3,5-triisopropylbenzene) having critical molecular diameters smaller and larger than the openings of the zeolite micropores. Our experimental data unambiguously show that, in contrast to what is usually assumed in the literature, the intracrystalline mesopores do not significantly affect intracrystalline diffusion in USY. This result indicates that the intracrystalline mesopores of USY zeolite do not form a connected network, which would allow diffusion through crystals only via mesopores.

## Introduction

Zeolites represent an important class of porous materials that have found numerous applications in catalysis due to their catalytic activity, framework stability, and a well-defined structure of micropores with a pore size around 1 nm.[1] In particular, Y-type zeolite is routinely used as a main, catalytically active component of fluid catalytic cracking catalysts. A major problem arising during catalytic applications of zeolites is related to transport limitations caused by a slow rate of diffusion of reactant and product molecules in zeolite micropores.[2−4] In the case of fluid catalytic cracking of crude oil many reactant molecules are either too large to penetrate the micropores of zeolite Y or can diffuse only very slowly in these micropores.[5] This problem was recognized a long time ago. To alleviate it, various types of postsynthesis treatment of Y-type zeolites such as steaming at elevated temperatures and acid leaching leading to an introduction of additional mesoporosity have been applied.[5−7] It is often assumed that the zeolite steaming, which is usually used to prepare USY for industrial applications, is very useful not only for increasing the hydrothermal stability of zeolites but also for enhancing the rate of intracrystalline diffusion due to formation of mesopores in the crystals. Mesopores are formed because of a partial collapse of the zeolite framework caused by the extraction of Al from the framework positions.[5] In addition to steaming, acid leaching can also be used to introduce mesopores into the zeolite framework. Recently, new knowledge about the mesopore structure of USY zeolites has become available through direct, 3-D observation of intracrystalline mesopores by using transmission electron microscopy (TEM).[8,9] The size of the mesopores was found to be distributed in a broad range between 2 and 50 nm. The TEM images have also shown that a significant part of the mesopores look more like cavities surrounded by micropores, rather than like channels with a direct connection to the outer crystal surface over the mesopore volume. In contrast to the pores of the latter type, the pores of the former type cannot be expected to lead to any significant increase of the mean intracrystalline diffusivity and of the related rate of molecular exchange between zeolite crystals and their surround-

[†] Universität Leipzig.
[‡] Cepsa Research Center.
[§] SINTEF Materials and Chemistry.
[||] Grace GmbH & Co. KG.
[⊥] University of Stuttgart.

(1) Baerlocher, C.; Meier, W. M.; Olson, D. H. *Atlas of Zeolite Framework Types*, 5 ed.; Elsevier: Amsterdam, 2001.
(2) Kärger, J.; Ruthven, D. M. *Diffusion in Zeolites and Other Microporous Solids*; Wiley & Sons: New York, 1992.
(3) Chen, N. Y.; Degnan, T. F.; Smith, C. M. *Molecular Transport and Reaction in Zeolites*; VCH: New York, 1994.
(4) Kärger, J.; Vasenkov, S.; Auerbach, S. M. Diffusion in Zeolites. In *Handbook of Zeolite Science and Technology*; Auerbach, S. M., Carrado, K. A., Dutta, P. K., Eds.; Marcel Dekker: New York, Basel, 2003; pp 341−423.
(5) *Fluid Catalytic Cracking V: Materials and Technological Innovations*; Ocelli, M. L., O'Connor, P., Eds.; Elsevier: Amsterdam, 2001.
(6) Müller, M.; Harvey, G.; Prins, R. *Microporous Mesoporous Mater*. **2000**, *34*, 135−147.
(7) Groen, J. C.; Jansen, J. C.; Moulijn, J. A.; Pérez-Ramírez, J. *J. Phys. Chem. B* **2004**, *108*, 13062−13065.
(8) Janssen, A. H.; Koster, A. J.; de Jong, K. P. *Angew. Chem., Int. Ed*. **2001**, *40*, 1102−1104.
(9) Janssen, A. H.; Koster, A. J.; de Jong, K. P. *J. Phys. Chem. B* **2002**, *106*, 11905−11909.

ings. Thus, the TEM data raise some doubts about the assumption that the diffusion rate may be significantly enhanced in zeolite USY in comparison to that of the parent zeolite Y. Although the TEM studies are clearly very useful for a clarification of the influence of mesopores on intracrystalline diffusion, they are unable to provide quantitative information on the extent of such influence on various relevant length scales. In particular, the relation between the crystal size and the length scale, where the micropore diffusion determines the diffusion rate in a macroscopic USY sample, can be obtained only by direct diffusion measurements. Additionally, monitoring diffusion in a macroscopic sample (viz. a zeolite bed) provides information about the average, characteristic diffusion properties, which might be different from those deduced on the basis of studies of mesopore systems in selected parts of several selected crystals. Here we report the results of a direct study of molecular diffusion in zeolite Y before and after hydrothermal treatment leading to the formation of USY zeolite. The diffusivities have been measured by using the pulsed field gradient (PFG) NMR technique[2,10−12] for a broad range of molecular displacements, including displacements much smaller than and comparable with the size of individual crystals. To characterize the connectivity of intracrystalline mesopores with the external crystal surface, the diffusion measurements have been performed with adsorbate molecules of different sizes (i.e., those that can easily penetrate into both zeolite micropores and mesopores and those that can freely access only mesopores). These studies have been made possible due to recent advances in PFG NMR the technique[13] and in the synthesis of large (around 3 $\mu$m) crystals of Y-type zeolite.[14]

## Experimental Section

PFG NMR is based on the dependence of the Larmor frequency, which can be understood as the frequency of the rotation of spins around the direction of the applied magnetic field, on the amplitude of the applied field.[2,10−12] Superimposing a large constant magnetic field by an inhomogeneous field (i.e., so-called magnetic field gradient pulses), we can label the positions of the spins by the Larmor frequency and hence also by the phases accumulated due to the rotation with the Larmor frequency in the local field. The dependence of the accumulated phase on the spin position is of crucial importance for the measured PFG NMR signal (spin−echo). If the molecules where the spins are located do not change their positions during the time of diffusion measurements, the signal will retain its maximum value. However, if there was a displacement of the molecules during this time interval, the measured spin−echo signal will lose part of its value. The resulting signal attenuation ($\Psi$) for the case of normal (i.e., Fickian) diffusion obtained with the 13-interval PFG NMR sequence may be presented as[15]

$$\Psi = \exp(-4\gamma^2\delta^2 g^2 Dt) \qquad (1)$$

where $D$ is the diffusivity, $t$ is the effective diffusion time, $\delta$ denotes the duration of the applied gradient pulses with the amplitude $g$, and $\gamma$ is the gyromagnetic ratio. The 13-interval PFG NMR sequence has been chosen for the present study because it allows suppressing distortions of the PFG NMR results by internal magnetic field inhomogeneities (i.e., internal magnetic field gradients) induced by susceptibility variations in heterogeneous samples.[15] To obtain diffusivity, the attenuation of the PFG NMR signal was measured as a function of the amplitude of the applied field gradient ($g$), keeping all other parameters of the pulse sequence constant. Diffusion measurements have been performed by using the home-built PFG NMR spectrometer FEGRIS 400 operating at a $^1$H resonance frequency of 400 MHz.[13] The maximum amplitude of the pulsed field gradients was 35 T/m. The diffusion time was varied in the range between 2.7 and 300 ms to obtain diffusivities in a broad range of the mean square displacements. The values of the mean square displacements were calculated by applying the Einstein relation

$$\langle r^2(t)\rangle = 6Dt \qquad (2)$$

The effective diffusion time was determined as discussed in refs 16 and 17.

The PFG NMR diffusion measurements have been carried out with the samples of USY zeolite and of the parent zeolite Y with a mean crystal size of around 3 $\mu$m. The latter sample was prepared by ammonium-ion exchange of zeolite NaY (Si/Al = 3.4).[14] The USY zeolite was obtained by steaming the ammonium-ion exchanged zeolite Y under the pressure of water vapor of 1 bar at 873 K for 5 h. Figure 1 shows scanning electron microscopic images of the samples obtained by CS44 electron microscope manufactured by CamScan. The results of the measurements of the nitrogen adsorption isotherms for these samples are presented in Table 1. The measurements have been performed by using Quantachrome Autosorb-1 instrument. The surface areas and pore volumes in Table 1 were determined by using t-plots according to the "de Boer method".[18] The total pore volume has been calculated for $p/po = 0.99$. The data in Table 1 indicate that, as expected, the zeolite ultrastabilization by steaming leads to an increase

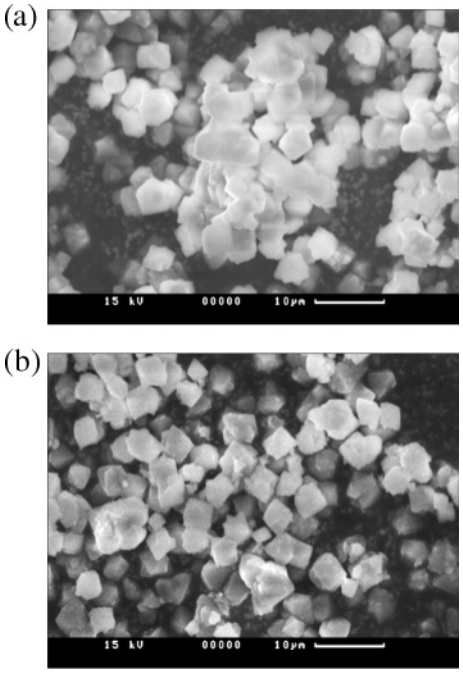


***Figure 1.*** Scanning electron microscopic images of the ammonium-ion exchanged zeolite Y (a) and of the USY (b) produced by steaming of the former zeolite under the pressure of water vapor of 1 bar at 873 K for 5 h.

(10) Callaghan, P. T. *Principles of NMR Microscopy*; Clarendon Press: Oxford, 1991.
(11) Kimmich, R. *NMR Tomography, Diffusometry, Relaxometry*; Springer: Berlin, 1997.
(12) Blümich, B. *NMR Imaging of Materials*; Clarendon Press: Oxford, 2000.
(13) Galvosas, P.; Stallmach, F.; Seiffert, G.; Kärger, J.; Kaess, U.; Majer, G. *J. Magn. Reson.* **2001**, *151*, 260−268.
(14) Berger, C.; Gläser, R.; Rakoczy, R. A.; Weitkamp, J. *Microporous Mesoporous Mater.* **2005**, *83*, 333−344.
(15) Cotts, R. M.; Hoch, M. J. R.; Sun, T.; Markert, J. T. *J. Magn. Reson.* **1989**, *83*, 252−266.
(16) Fordham, E. J.; Mitra, P. P.; Latour, L. L. *J. Magn. Reson.* **1996**, *121*, 187−192.
(17) Vasenkov, S.; Böhlmann, W.; Galvosas, P.; Geier, O.; Liu, H.; Kärger, J. *J. Phys. Chem. B* **2001**, *105*, 5922−5927.
(18) de Boer, J. H.; Lippens, B. C.; Linsen, B. G.; Broekhoff, J. C. P.; van den Heuvel, A.; Osinga, Th. J. *J. Colloid Interface Sci.* **1966**, *21*, 405.

***Table 1.*** Results from Nitrogen Adsorption on the Ammonium-Ion Exchanged Y and USY Zeolites

| sample | total specific surface area ($m^2/g$) | specific surface area of micropores ($m^2/g$) | specific surface area of mesopores ($m^2/g$) | specific volume of micropores (mL/g) | specific volume of mesopores (mL/g) |
|---|---|---|---|---|---|
| ammonium-ion exchanged Y | 763 | 731 | 32 | 0.28 | 0.07 |
| USY | 688 | 624 | 64 | 0.24 | 0.17 |

of the specific surface area and volume of mesopores and to a slight decrease of the specific microporous surface area and volume.

1,3,5-Triisopropylbenzene (1,3,5-TIPB; Aldrich, 96%) and *n*-octane (Aldrich, 99%) were chosen as probe molecules for diffusion studies. The molecules of the first type have a critical diameter of around 0.95 nm,[19] which is much larger than the size of the supercage windows of Faujasite-type zeolite (around 0.74 nm).[1] Hence, these molecules are expected either to have extremely small diffusivities in the micropore system of zeolite Y or to have been unable to penetrate into the micropores at all. The molecules of the second type can freely access both the micropores and mesopores.

For the preparation of the PFG NMR samples, around 300 mg of the zeolite was introduced into the NMR tube. Then the tube was connected to the vacuum system, and the sample was activated by keeping it under high vacuum (less than $10^{-2}$ mbar) at 673 K for around 40 h. This activation procedure ensures that the zeolite crystals are essentially adsorbate-free by the end of the activation. It is also expected to convert most of the $NH_4Y$ zeolite into HY zeolite. The loading with *n*-octane was achieved by freezing a certain amount of the adsorbate from the calibrated volume of the vacuum system into the sample tube with the activated zeolite. The loading of *n*-octane was in all cases 0.65 mmol/g. In this case, more than 50% of the available micropore volume is expected to be filled with the adsorbate. The loading with 1,3,5-TIPB was carried out by introducing the liquid adsorbate into the PFG NMR tube with the activated zeolite by using a syringe. The amount of 1,3,5-TIPB (around $1.2 \times 10^{-3}$ mL of 1,3,5-TIPB per 1 mg of adsorbate-free zeolite Y) was chosen in such a way that the zeolite sample in the tube was completely covered with the liquid. This condition ensures that all intracrystalline mesopores, which can be accessed from the external crystal surface, are completely filled with the liquid. Upon loading, the NMR tubes were sealed and separated from the vacuum system.

## Results and Discussion

Figure 2 shows the measured dependencies of the effective *n*-octane diffusivities on the root-mean-square displacement in the ammonium-ion exchanged Y and USY zeolites. The diffusivities were obtained from the corresponding slopes of the PFG NMR attenuation curves, which were found to comply in all cases with eq 1. The data in Figure 2 indicate that the measured diffusivities decrease with the increasing root-mean-square displacement. It is seen that in the semilogarithmic presentation of Figure 2 the shape of the dependencies for any particular sample remains essentially the same at different temperatures. This behavior can be attributed to the restriction of the diffusion of guest molecules by the size of the zeolite crystals and/or crystal agglomerates.[2]

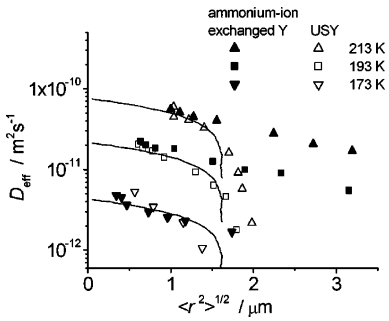


***Figure 2.*** Dependencies of the effective diffusivities on the mean square displacements measured for *n*-octane by PFG NMR (points) and those obtained by the dynamic Monte Carlo simulations (lines) for a cubic lattice with a size $2.3 \times 2.3 \times 2.3$ $\mu m^3$. The boundaries of the simulation lattice were assumed to be impenetrable for diffusing molecules.

In the considered situation, the molecular displacements are so large that during the diffusion time many molecules can reach the crystal (agglomerate) external surface. Once they reach the surface, the molecules are often reflected back to the inner part of the crystals due to either a large difference between the potential energy in the intracrystalline volume and in the surrounding gas phase or a high concentration of structural defects, which are expected to exist on the external surface of zeolite crystals. It is interesting to note that the mean separation between the restrictive boundaries (i.e., the mean size of the zeolite crystals and of the crystal agglomerates) does seem to be different in different samples. This is demonstrated by the observation that the shape of the dependencies in Figure 2 is different for the ammonium-ion exchanged and ultrastabilized samples. In the latter sample, the measured diffusivities rapidly decrease for root-mean-square displacements around 1.5 $\mu$m or larger, while in the former one the pace of the diffusivity decrease remains much more moderate even for root-mean-square displacements significantly larger than 1.5 $\mu$m. This observation can be understood by assuming that the mean size of the domains where the unrestricted intracrystalline diffusion occurs is larger in the ammonium-ion exchanged Y than in the USY. To estimate the size of these domains in the USY sample, the PFG NMR diffusion data in Figure 2 were fitted by the corresponding results of the dynamic Monte Carlo simulations. The simulations were carried out by assuming that all the domains can be presented as cubes of the same size with ideally reflecting boundaries. The diffusion was modeled by random walks performed on a cubic lattice of size $200 \times 200 \times 200$ as described in our recent articles.[17,20] These simulations are analogous to the corresponding numerical solution of Fick's second law-type equations with constant diffusivities, reflecting boundaries and equal initial concentration in all lattice sites. The condition of reflecting boundaries is used to simulate the situation frequently encountered in real zeolite systems when the rate of molecular desorption is controlled by a low (but nonzero) permeability of the surface layer of zeolite crystals.[4] For sufficiently small times used in our simulations, very low and zero permeabilities are expected to produce essentially the same results. Lines in Figure 2 show the best fit results

(19) Bhatia, S. *Zeolite Catalysis, Principles and Applications*; CRC Press: Boca Raton, FL, 1990; Vols. 7−18.

(20) Vasenkov, S.; Karger, J. *Microporous Mesoporous Mater*. **2002**, *55*, 139−145.

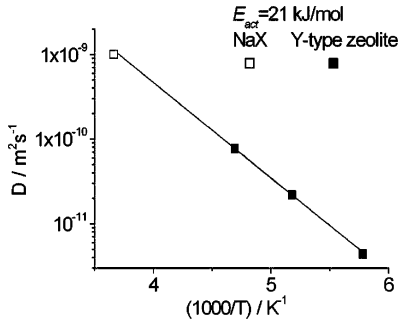


***Figure 3.*** Temperature dependence of the *n*-octane diffusivity in Y-type zeolite obtained by the extrapolation of the simulation results in Figure 2 to small displacements (filled points). Also shown for comparison is the unrestricted intracrystalline diffusivity of *n*-octane measured by PFG NMR in zeolite NaX for similar *n*-octane loading (open point). Line shows the result of the fitting of the diffusivities in Y-type zeolite by the Arrhenius law.

corresponding to an edge size of the simulation lattice of 2.3 $\mu$m. This value is in a good agreement with a mean size of USY crystallites (2.7 $\pm$ 0.6 $\mu$m), which was estimated from the images of the sample obtained by scanning electron microscopy (see examples in Figure 1). The images of the USY sample failed to provide any evidence of frequent crystal agglomeration (Figure 1b). Hence, in agreement with that discussed above, the mean separation between the diffusion restrictions is expected to be determined by the mean crystallite size. At the same time, many crystal agglomerates seem to exist in the ammonium-ion exchanged sample (Figure 1a). Crystal agglomeration in the latter sample is likely to increase the mean size of the domains where the intracrystalline diffusion may occur. This explains the diffusion data in Figure 2 for the ammonium-ion exchanged zeolite Y showing only a relatively slow decrease of the effective diffusivities with increasing displacements, even when the root-mean-square displacements become larger than the crystallite size. For root-mean-square displacements, which are significantly smaller than the crystallite size, good agreement between the measured diffusivities was observed in both samples at all temperatures used (Figure 2).

Figure 3 shows the temperature dependence of the unrestricted intracrystalline diffusivity, which was obtained by the extrapolation of the simulation curves in Figure 2 to $\sqrt{\langle r^2(t)\rangle} = 0$. This temperature dependence can be well described by the Arrhenius law $D = D_0 \exp(-E_{act}/RT)$ with $E_{act} = 21$ kJ/mol. The values of the *n*-octane diffusivity in the Y-type zeolites extrapolated to higher temperatures by using the Arrhenius law with $E_{act} = 21$ kJ/mol were found to be close to the corresponding diffusivity of *n*-octane in NaX measured by PFG NMR[2] (Figure 3).

At the same time, at least 4 orders of magnitude lower apparent diffusivities of *n*-octane in USY were recently measured by the zero-length column (ZLC) method.[21] The discrepancy between the results reported in this article and those obtained by ZLC might be related to the fact that the apparent diffusivities measured by the latter technique can be significantly reduced by the existence of the transport resistances on the crystallite surface.

All the data discussed earlier in this article indicate that mesopores formed by the zeolite steaming are essentially of no influence for the intracrystalline diffusion of *n*-octane in the studied sample of USY zeolite. *n*-Octane molecules can easily penetrate both the zeolite micropores and mesopores. Later in this article we report the results of the PFG NMR diffusion measurements performed with another type of probe molecule (i.e., 1,3,5-TIPB), which is too large to be easily adsorbed into the micropores of Y-type zeolite but, at the same time, is sufficiently small to access mesopores. For these measurements, zeolite beds were saturated with liquid 1,3,5-TIPB, ensuring the condition that all mesopores accessible from the external surface of zeolite crystals are filled with the liquid adsorbate.

(21) Cavalcante, C. L., Jr.; Silva, N. M. *Adsorption* **2003**, *9*, 205−212.

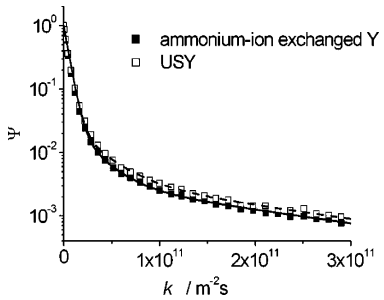


***Figure 4.*** PFG NMR attenuation curves for 1,3,5-TIPB in the Y-type zeolites for a diffusion time 10 ms at 298 K. Lines show the best fit results by using eq 3 with $N = 3$. The best fit parameters are presented in Table 2.

***Table 2.*** Best Fit Parameters Obtained by Fitting the Experimental Attenuation Curves in Figure 4 by Eq 3 with $N = 3$ and the Corresponding Volumetric Fractions of Liquid 1,3,5-TIPB Having Diffusivities $D_{1,2,3}$

| best fit parameters, specific volumes | ammonium-ion exchanged Y | USY |
|---|---|---|
| $P_1$ | $0.97 \pm 0.003$ | $0.97 \pm 0.003$ |
| $D_1$ (m$^2$/s) | $(2 \pm 0.5) \times 10^{-10}$ | $(2 \pm 0.5) \times 10^{-10}$ |
| $P_2$ | $(2.7 \pm 0.3) \times 10^{-2}$ | $(2.5 \pm 0.3) \times 10^{-2}$ |
| $D_2$ (m$^2$/s) | $(4 \pm 1) \times 10^{-11}$ | $(4 \pm 1) \times 10^{-11}$ |
| $P_3$ | $(3 \pm 0.7) \times 10^{-3}$ | $(4 \pm 1) \times 10^{-3}$ |
| $D_3$ (m$^2$/s) | $(4 \pm 1) \times 10^{-12}$ | $(4 \pm 1) \times 10^{-12}$ |
| $v_1$ (mL/g) | $1.1 \pm 0.5$ | $1.0 \pm 0.5$ |
| $v_2$ (mL/g) | $(3 \pm 1.7) \times 10^{-2}$ | $(2 \pm 1.5) \times 10^{-2}$ |
| $v_3$ (mL/g) | $(4 \pm 3) \times 10^{-3}$ | $(4 \pm 3) \times 10^{-3}$ |

The PFG NMR attenuation curves for 1,3,5-TIPB in the samples with the ammonium-ion exchanged Y and USY zeolites exhibit pronounced nonexponential behavior (Figure 4). This result can be explained by assuming the existence of several fractions of adsorbate molecules having different diffusivities. In this case, the attenuation curves may be presented as a sum of the exponential terms of the type written in the right part of eq 1

$$\Psi = \sum_{i=1}^{n=N} P_i \exp(-kD_i) \qquad (3)$$

where $k = 4\gamma^2\delta^2g^2t$ and $P_i$ is the probability of finding molecules with the diffusivity $D_i$.

Fitting of the experimental attenuation curves by using eq 3 revealed that the smallest number of the exponential terms (viz. $N$ in eq 3) needed to get a satisfactory agreement between the calculated and the experimental curves is three. Lines in Figure 4 show the best fit results for $N = 3$ with the best fit parameters presented in Table 2. This table also shows the values of the specific volume ($v_i$) of the liquid 1,3,5-TIPB having diffusivity $D_i$ ($i = 1, 2, 3$). The former values were estimated from the

best fit results for $P_i$ by using the known weights of 1,3,5-TIPB and the zeolite introduced into the PFG NMR tubes. For this estimate, it was assumed that the values of $P_2$ and $P_3$ corresponding to smaller diffusivities were not significantly affected (i.e., reduced) by an additional weighting over NMR transverse relaxation time ($T_2$) and/or by the molecular exchange with the adsorbate fraction having larger diffusivity ($D_1$).[22]

It is seen in Table 2 that the values of $D_i$, $P_i$, and $v_i$ ($i = 1$, 2, 3) are essentially the same for both samples. This observation suggests that, in complete analogy with the data obtained for *n*-octane, the mesopores formed by steaming zeolite Y have no significant influence on diffusion of 1,3,5-TIPB. Additional PFG NMR diffusion measurements performed with the PFG NMR tube filled only with liquid 1,3,5-TIPB revealed diffusivity, which was in excellent agreement with the value of $D_1$. This result allows us to assign $D_1$ to the unrestricted diffusivity of liquid 1,3,5-TIPB in the intercrystalline volume of the sample (i.e., in the volume formed by the gaps between the zeolite crystals and/or crystal agglomerates and in the volume on top of the zeolite bed in the PFG NMR tube). The diffusivities $D_2$ and $D_3$ can be assigned to the diffusion coefficients of 1,3,5-TIPB in various types of mesopores and/or to the intracrystalline diffusivities of 4% of impurities present in 1,3,5-TIPB. At least some of the mesopores mentioned above might be located in a small amount of nonzeolitic impurities present in the sample. Comparison of the data in Tables 1 and 2 shows that the values of the total specific volume of the adsorbate having diffusivities $D_2$ and $D_3$ are essentially the same in both samples and several times smaller than the specific volume of mesopores in USY. Hence, even if some of the intracrystalline mesopores in the USY zeolite are accessible for 1,3,5-TIPB and the diffusion in these mesopores contributes to the diffusivities $D_2$ and $D_3$, these mesopores represent only a small fraction of all mesopores in the USY crystals.

On the basis of all the PFG NMR data discussed above, we can conclude that intracrystalline diffusion of guest molecules is essentially unaffected by mesopores in USY. This result can be understood by assuming that mesopores in USY crystals do not form a connected (i.e., percolation) network allowing diffusion of guest molecules through the crystals via only mesopores. Creation of such diffusion pathway can be expected to lead to an order-of-magnitude increase in the characteristic intracrystalline diffusivities in comparison to the mesopore-free crystals. This expectation is related to the possibility for guest molecules to diffuse out of zeolite crystals via only mesopores (i.e., very fast) as soon as they reach the mesopore volume for the first time. In contrast, if this diffusion pathway does not become available, only moderate increase in the intracrystalline diffusivities can be expected due to generation of mesopores. Under such conditions, the diffusion process can be described as a consecutive diffusion via mesopores and via zeolite micropores. The latter process is, obviously, the slowest one. Hence, the diffusion via zeolite micropores is expected to limit the rate of the overall diffusion.

The most important practical consequence of the results reported above is the conclusion that zeolite dealumination is apparently not a very efficient way of reducing transport limitations caused by small pore sizes in zeolites. This conclusion emphasizes the importance of recent efforts aiming at fabrication of ordered mesoporous zeolites by using advanced techniques such as the template method.[23−27] This method is based on synthesis of zeolite nanocrystals in mesopores of an inert matrix, which is followed by the matrix removal.

**Acknowledgment.** This work has been done under coordination of Leipzig University, Germany, in the framework of the "TROCAT" project (Contract G5RD-CT-2001-00520), which is funded by the European Community under the "Competitive and Sustainable Growth" Program. We are grateful to the following project participants for most stimulating discussions of the results: Prof. D. Theodorou and Dr. G. K. Papadopoulos (National Technical University of Athens, Greece); Dr. M. Kočiřík, Dr. A. Zikánová, Ms. H. Jirglová (Heyrovský Institute of Physical Chemistry, Czech Republic); and Prof. E. W. Hansen (University of Oslo, Norway).

JA053134R

(22) The former assumption is supported by the experimental observation that the best fit values of the parameters $P_1$ and $P_2$ in eq 3 are only insignificantly reduced for the attenuation curves obtained under the condition when the total time in the PFG NMR sequence, during which the signal decays with the transverse relaxation time, is increased by a factor of 2 in comparison with that normally used for the measurements. We can also rule out the possibility that molecular exchange strongly affects the apparent values of $P_2$ and $P_3$ based on the following two results: (i) these values were found to change only very slowly with increasing diffusion time and (ii) the root-mean-square displacements of the adsorbate fractions having diffusivities $D_2$ and $D_3$ at the smallest diffusion time used in the measurements (10 ms) were found to be smaller, correspondingly, by around a factor of 2 and a factor of 5 than the mean size of the zeolite crystals.

(23) Jacobsen, C. J. H.; Madsen, C.; Houzvicka, J.; Schmidt, I.; Carlsson, A. *J. Am. Chem. Soc*. **2000**, *122*, 7116−7117.
(24) Tao, Y.; Kanoh, H.; Kaneko, K. *J. Am. Chem. Soc.* **2003**, *125*, 6044−6045.
(25) Kim, S.-S.; Shah, J.; Pinnavaia, T. J. *Chem. Mater*. **2003**, *15*, 1664−1668.
(26) Tao, Y.; Kanoh, H.; Kaneko, K. *J. Phys. Chem. B* **2003**, *107*, 10974−10976.
(27) Cepak, V. M.; Hulteen, J. C.; Che, G. L.; Jirage, K. B.; Lakshmi, B. B.; Fisher, E. R.; Martin, C. R.; Yoneyama, H. *Chem. Mater*. **1997**, *9*, 1065−1067.